ISSN 1064-2269, Journal of Communications Technology and Electronics, 2015, Vol. 60, No. 8, pp. 852–859. © Pleiades Publishing, Inc., 2015.
Original Russian Text © A.P. Trifonov, Yu.N. Pribytkov, O.V. Chernoyarov, B.B. Mikhailov, 2015, published in Radiotekhnika i Elektronika, 2015, Vol. 60, No. 8, pp. 805–812.

STATISTICAL RADIOPHYSICS

Estimating the Image Area with Unknown Parameters of the Image and Background

A. P. Trifonov[a], Yu. N. Pribytkov[a], O. V. Chernoyarov[b], and B. B. Mikhailov[c]

[a] *Voronezh State University, Universitetskaya pl. 1, Voronezh, 394007 Russia*
[b] *National Research University MPEI, ul. Krasnokazarmennaya 14, Moscow, 111250 Russia*
[c] *Bauman Moscow State Technical University, Vtoraya Baumanskaya ul. 5/1, Moscow, 105005 Russia*
e-mail: trifonov@phys.vsu.ru

Received February 18, 2015

Abstract—The characteristics of quasi-likelihood and maximum-likelihood estimates of the image area are obtained in the case when the regular components and intensities of the image and applicative background are unknown. The influence of the prior uncertainty in these parameters on the accuracy of estimating the area is analyzed.

DOI: 10.1134/S1064226915080185

As is known, one of the main problems solved by machine vision systems is the estimation of parameters of volumetric objects from their images [1, 2]. One of the parameters requiring exact estimation in problems of the analysis of irregularities of images with a stochastic structure is the area of irregularities of the image. When developing practically implementable algorithms, it is necessary to have predictable characteristics of area estimation algorithms and analyze the influence of the prior uncertainty in the parameters of the images of the object and underlying surface on the quality of the estimate. Such analysis can be performed with the use of pertinent models of the image and background. One of such models, appropriate for describing objects with a stochastic texture, may be the model in the form of a Gaussian random field [3–5], which is widely used for the synthesis of optimal algorithms for finding and filtration of images [4]. This model enables one to describe textures of images and background by specifying their space correlation functions. In addition, this model is a special case of a generalized Gaussian model [6] describing a wide class of real-life images.

The problem of estimating the area of a Gaussian volumetric object observed on a Gaussian background was considered in [7] in the case when the parameters of the image and background are known. The aim of the present work is the synthesis and analysis of the efficiency of area estimation algorithms when the regular components and intensities of the image and background are unknown.

Assume that the observed data $x(\vec{r})$ are a realization of a random field and occupy a two-dimensional region G with the area χ_G. Here, $\vec{r} = (r_1, r_2)$ is the radius vector of a point on a plane belonging to G. The field $x(\vec{r})$ contains the useful image of an object $s(\vec{r})$, the spatial noise $n(\vec{r})$, and the background radiation $\nu(\vec{r})$. This radiation is caused by the scattering of the sensing signal by the underlying surface, on which the object to be detected is found. For taking into account the shading of the background, which takes place in practice, we will use an applicative model of the interaction between the image and the background [5], in which the observed realization can be represented in the form

$$x(\vec{r}) = I_s(\vec{r},\chi_0)s(\vec{r}) + I_\nu(\vec{r},\chi_0)\nu(\vec{r}) + n(\vec{r}). \quad (1)$$

Here, $I_s(\vec{r},\chi) = I(\vec{r},\Omega_s(\chi))$ and $I_\nu(\vec{r},\chi) = I(\vec{r},\Omega_\nu \times (\chi_G - \chi))$ are the indicators of the regions occupied by the image $\Omega_s(\chi)$ and the background $\Omega_\nu(\chi_G - \chi)$; $I(\vec{r},\Omega(\chi)) = 1$ if $\vec{r} \in \Omega(\chi)$ and $I(\vec{r},\Omega(\chi)) = 0$ if $\vec{r} \notin \Omega(\chi)$ is the indicator of the region $\Omega(\chi)$, having the area χ; and χ_0 is the true value of the unknown area, which can take the values from the interval $[\chi_{\min}, \chi_{\max}]$.

Henceforward we will assume that the image $s(\vec{r})$ and the background $\nu(\vec{r})$ are homogeneous statically mutually independent Gaussian fields with the regular components (mathematical expectations) a_s and a_ν and the correlation functions $B_s(\vec{r})$ and $B_\nu(\vec{r})$. We will also assume that the spectral densities of the image, $G_s(\vec{\omega}) = \int_{-\infty}^{\infty} B_s(\vec{r})\exp(-j\vec{\omega}\,\vec{r})\,d\vec{r}$, and the background, $G_\nu(\vec{\omega}) = \int_{-\infty}^{\infty} B_\nu(\vec{r})\exp(-j\vec{\omega}\,\vec{r})\,d\vec{r}$, are constant in the spatial frequency ranges ω_s and ω_ν, respectively. Out-

side these ranges, the spectral densities of the image and background are zero, i.e., $G_s(\vec{\omega}) = g_s I(\vec{\omega}, \omega_s)$ and $G_\nu(\vec{\omega}) = g_\nu I(\vec{\omega}, \omega_\nu)$, where $I(\vec{\omega}, \omega) = 1$ for $\vec{\omega} \in \omega$ and $I(\vec{\omega}, \omega) = 0$ for $\vec{\omega} \notin \omega$, $g_s = G_s(0)$, and $g_\nu = G_\nu(0)$. We assume that the spatial noise $n(\vec{r})$ is mutually independent with the image and the background and is a realization of a centered white Gaussian noise with zero mean and single-sided spectral density N_0.

Thus, the problem is to estimate the unknown area χ_0 of the image with unknown components a_s and a_ν and relative intensities of the image, $q_s = 2g_s/N_0$, and background, $q_\nu = 2g_\nu/N_0$.

For estimating the unknown area according to the statistical decision theory [8], we find the unknown form of the likelihood ratio functional (LRF) for testing hypothesis (1) against the alternative $x(\vec{r}) = n(\vec{r})$. In this case we assume that the areas of the image and background substantially exceed the area of their spatial correlation, i.e.,

$$\mu_s = \chi_{\min} S_{\omega s}/(2\pi)^2 \gg 1, \quad \mu_b = \chi_{\min} S_{\omega\nu}/(2\pi)^2 \gg 1, \quad \mu_\nu = (\chi_G - \chi_{\max}) S_{\omega\nu}/(2\pi)^2 \gg 1, \tag{2}$$

where $S_{\omega s}$ and $S_{\omega\nu}$ are the areas of the regions ω_s and ω_ν, respectively. Then, extending the results of [9] to the case of an unknown area, we approximate the logarithm of the LRF (log-LRF) as follows:

$$L(a_s, q_s, a_\nu, q_\nu, \chi) = L_s(a_s, q_s, \chi) + L_\nu(a_\nu, q_\nu, \chi), \tag{3}$$

where

$$L_s(a_s, q_s, \chi) = \frac{1}{N_0} Y_s(\chi) - \frac{1}{N_0(1+q_s)} \times \left[Y_s(\chi) - 2a_s X_s(\chi) + a_s^2 \chi \right] - \frac{\mu_s \chi}{2\chi_{\min}} \ln(1+q_s), \tag{4}$$

$$L_\nu(a_\nu, q_\nu, \chi) = \frac{1}{N_0} Y_\nu(\chi) - \frac{1}{N_0(1+q_\nu)} \left[Y_\nu(\chi) - 2a_\nu X_\nu(\chi) + a_\nu^2 (\chi_G - \chi) \right] - \frac{\mu_\nu (\chi_G - \chi)}{2(\chi_G - \chi_{\max})} \ln(1+q_\nu) \tag{5}$$

are the log-LRFs for the regions presumably occupied by the image and the background. In expressions (4) and (5) we use the following notation:

$$X_s(\chi) = \int_{\Omega_s(\chi)} x(\vec{r})\, d\vec{r}, \quad X_\nu(\chi) = \int_{\Omega_\nu(\chi_G - \chi)} x(\vec{r})\, d\vec{r},$$
$$Y_s(\chi) = \int_{\Omega_s(\chi)} y_s^2(\vec{r})\, d\vec{r}, \quad Y_\nu(\chi) = \int_{\Omega_\nu(\chi_G - \chi)} y_\nu^2(\vec{r})\, d\vec{r},$$

where $y_s(\vec{r})$ and $y_\nu(\vec{r})$ are the signals at the outputs of the spatial filters whose transfer functions satisfy the conditions $|H_s(\vec{\omega})|^2 = I(\vec{\omega}, \tilde{\omega}_s)$ and $|H_\nu(\vec{\omega})|^2 = I(\vec{\omega}, \tilde{\omega}_\nu)$, respectively. Expressions (3)–(5) show that, in order to form the log-LRF, one has to obtain a linear combination of four functions: $Y_s(\chi)$, $Y_\nu(\chi)$, $X_s(\chi)$, and $X_\nu(\chi)$, which depend on the unknown value of the area. In this case, to form $Y_s(\chi)$ and $Y_\nu(\chi)$, one should apply two linear filters: the frequency characteristic of one of them is determined by the spectral density of the image and that of the other one, by the spectral density of the background. The signals at the outputs of these filters should be squared and integrated over the region occupied by the image. In addition, it is necessary to form the integrals $X_s(\chi)$ and $X_\nu(\chi)$ of the accepted realization of the observed data over the region occupied by the image and background.

At first, let us consider the quasi-likelihood approach to estimating the unknown area when the mathematical expectations of the image and background intensities are unknown. To this end, we replace the unknown values of the parameters a_s, q_s, a_ν, and q_ν in (3) by some predicted values a_s^*, q_s^*, a_ν^*, and q_ν^*, generally different from the true values a_{s0}, q_{s0}, $a_{\nu 0}$, and $q_{\nu 0}$. Then the estimate of the unknown area is defined as the position of the absolute maximum of $L(a_s^*, q_s^*, a_\nu^*, q_\nu^*, \chi)$:

$$\hat{\chi}_{\mathrm{QLE}} = \arg\max_{\chi} L(a_s^*, q_s^*, a_\nu^*, q_\nu^*, \chi).$$

According to [9, 10], as $\mu_s \to \infty$ and $\mu_\nu \to \infty$, the distribution of functionals (4) and (5) at a fixed unknown parameter χ tends to the Gaussian one. Henceforward we will assume that the minimum image area $\chi_{\min}$ and the maximum background area $\chi_G - \chi_{\max}$ are so large that $\mu_s \gg 1$ and $\mu_\nu \gg 1$. Then, as was shown in [7], in the vicinity of the true value of the parameter, χ_0, the log-LRF $L(a_s^*, q_s^*, a_\nu^*, q_\nu^*, \chi)$ (3) as a function of the unknown area χ may be approximately considered a Gaussian Markov process. Using the method for calculating the characteristics of a Gaussian Markov process [9], we find the following expressions for the drift coefficient,

$$K_{1\mathrm{QLE}}(a_s^*, q_s^*, a_\nu^*, q_\nu^*, \chi) = \frac{1}{\chi_{\min}} \begin{cases} k_1(a_s^*, q_s^*, a_\nu^*, q_\nu^*), & \chi_{\min} \le \chi \le \chi_0, \\ -k_2(a_s^*, q_s^*, a_\nu^*, q_\nu^*), & \chi_0 < \chi \le \chi_{\max}, \end{cases} \tag{6}$$

and the diffusion coefficient,

$$K_{2\mathrm{QLE}}(a_s^*, q_s^*, a_\nu^*, q_\nu^*, \chi) = \frac{1}{\chi_{\min}} \begin{cases} d_1(a_s^*, q_s^*, a_\nu^*, q_\nu^*), & \chi_{\min} \le \chi \le \chi_0, \\ d_2(a_s^*, q_s^*, a_\nu^*, q_\nu^*), & \chi_0 < \chi \le \chi_{\max}, \end{cases} \tag{7}$$

of the process $L(a_s^*, q_s^*, a_\nu^*, q_\nu^*, \chi)$.

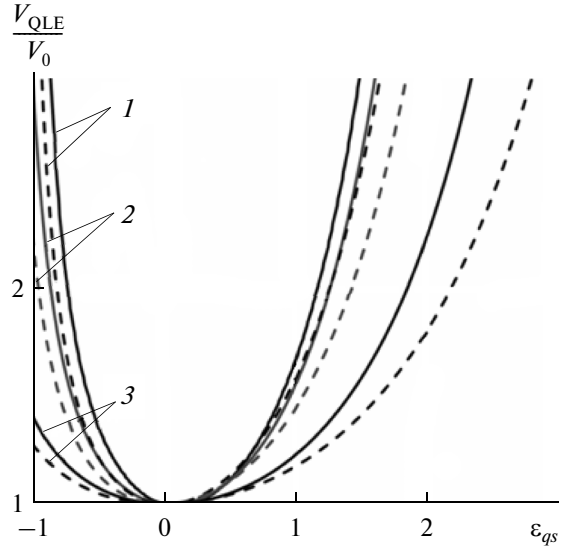

Fig. 1. The loss in the area estimation accuracy vs. presumed values of image intensity.

Here,

$$k_1(a_s^*,q_s^*,a_\nu^*,q_\nu^*)=\frac{\mu_s q_s^*(1+q_{s0})}{2\left(1+q_s^*\right)}-\frac{\mu_\nu q_\nu^*}{2\left(1+q_\nu^*\right)}$$
$$\times\frac{\chi_{\min}}{\chi_G-\chi_{\max}}\left(1+\varphi q_{s0}\sqrt{\frac{\mu_s}{\mu_b}}\right)+\frac{\chi_{\min}}{N_0}\left[\frac{(a_{s0}-a_\nu^*)^2}{1+q_\nu^*}\right. \quad (8)$$
$$\left.-\frac{(a_s^*-a_{s0})^2}{1+q_s^*}\right]-\frac{\mu_s}{2}\ln(1+q_s^*)+\frac{\mu_\nu\chi_{\min}}{2(\chi_G-\chi_{\max})}\ln(1+q_\nu^*),$$

$$k_2(a_s^*,q_s^*,a_\nu^*,q_\nu^*)=-\frac{\mu_s q_s^*}{2(1+q_s^*)}\left(1+\varphi q_{\nu0}\sqrt{\frac{\mu_b}{\mu_s}}\right)$$
$$+\frac{\mu_\nu\chi_{\min}}{2(\chi_G-\chi_{\max})}\frac{q_\nu^*(1+q_{\nu0})}{1+q_\nu^*}-\frac{\chi_{\min}}{N_0}\left[\frac{(a_{\nu0}-a_\nu^*)^2}{1+q_\nu^*}\right. \quad (9)$$
$$\left.-\frac{(a_s^*-a_{\nu0})^2}{1+q_s^*}\right]+\frac{\mu_s}{2}\ln(1+q_s^*)-\frac{\mu_\nu\chi_{\min}}{2(\chi_G-\chi_{\max})}\ln(1+q_\nu^*),$$

$$d_1(a_s^*,q_s^*,a_\nu^*,q_\nu^*)=\frac{1}{2(1+q_s^*)^2}$$
$$\times\left[\mu_s q_s^{*2}(1+q_{s0})^2+\frac{4\chi_{\min}}{N_0}(1+q_{s0})(a_{s0}q_s^*+a_s^*)^2\right]$$
$$+\frac{1}{2(1+q_\nu^*)^2}\left[\frac{\mu_\nu\chi_{\min}q_\nu^{*2}}{\chi_G-\chi_{\max}}\left(1+\varphi q_{s0}(2+q_{s0})\sqrt{\frac{\mu_s}{\mu_b}}\right)\right. \quad (10)$$
$$\left.+\frac{4\chi_{\min}}{N_0}(1+q_{s0})(a_{s0}q_s^*+a_\nu^*)^2\right],$$

$$d_2(a_s^*,q_s^*,a_\nu^*,q_\nu^*)=\frac{1}{2(1+q_\nu^*)^2}\left[\frac{\mu_\nu\chi_{\min}q_\nu^{*2}}{\chi_G-\chi_{\max}}\right.$$
$$\times(1+q_{\nu0})^2+\frac{4\chi_{\min}}{N_0}(1+q_{\nu0})(a_{\nu0}q_\nu^*+a_\nu^*)^2\Bigg]$$
$$+\frac{1}{2(1+q_s^*)^2}\left[\mu_s q_s^{*2}\left(1+\varphi q_{\nu0}(2+q_{\nu0})\sqrt{\frac{\mu_b}{\mu_s}}\right)\right. \quad (11)$$
$$\left.+\frac{4\chi_{\min}}{N_0}(1+q_{\nu0})(a_{\nu0}q_s^*+a_s^*)^2\right],$$

$\varphi=S_{\omega s\nu}/\sqrt{S_{\omega s}S_{\omega\nu}}$ is a coefficient determining the degree of overlapping of the regions occupied by the spectral densities of the useful image and the background, and $S_{\omega s\nu}$ is the area of overlapping of these regions. Then, following [9, 11], we estimate the conditional dispersion of the estimate of the area as

$$V_{\mathrm{QLE}}(a_s^*,q_s^*,a_\nu^*,q_\nu^*,\hat{\chi}|\chi_0)$$
$$\approx\chi_{\min}^2\left[\frac{2+6R+5R^2}{2z_2^4(1+R)^3}+\frac{R\left(5+6R+2R^2\right)}{2z_1^4(1+R)^3}\right], \quad (12)$$

where

$$R=k_2(a_s^*,q_s^*,a_\nu^*,q_\nu^*)d_1(a_s^*,q_s^*,a_\nu^*,q_\nu^*)\Big/k_1(a_s^*,$$
$$q_s^*,a_\nu^*,q_\nu^*)d_2(a_s^*,q_s^*,a_\nu^*,q_\nu^*),$$
$$z_1=k_1(a_s^*,q_s^*,a_\nu^*,q_\nu^*)\Big/\sqrt{d_1(a_s^*,q_s^*,a_\nu^*,q_\nu^*)},$$
$$\text{and } z_2=k_2(a_s^*,q_s^*,a_\nu^*,q_\nu^*)\Big/\sqrt{d_2(a_s^*,q_s^*,a_\nu^*,q_\nu^*)}.$$

Expression (12) makes it possible to estimate the influence of the inaccuracy of specifying the predicting values a_s^*, q_s^*, a_ν^*, q_ν^* of the unknown parameters on the area estimation accuracy. For example, Fig. 1 shows the loss in the area estimation accuracy, V_{QLE}/V_0, as a function of the ratio $\varepsilon_{qs}=(q_s^*-q_{s0})/q_{s0}$ for $q_\nu^*=q_{\nu0}$, $a_s^*=a_{s0}=a_\nu^*=a_{\nu0}$, $\mu_s=\mu_\nu=100$, $\varphi=0$, $\chi_{\max}/\chi_{\min}=10$, $\chi_G/\chi_{\min}=12$, $\chi_0/\chi_{\min}=5$, and $z_s=z_\nu=10$. Here, $V_{\mathrm{QLE}}=V_{\mathrm{QLE}}(a_s^*,q_s^*,a_\nu^*,q_\nu^*,\hat{\chi}|\chi_0)$ and $V_0=V_{\mathrm{QLE}}(a_{s0},q_{s0},a_{\nu0},q_{\nu0},\hat{\chi}|\chi_0)$ are the dispersion of area estimation at a prior known regular components and relative image and background intensities, $z_s^2=2a_{s0}^2\chi_{\min}/N_0$ and $z_\nu^2=2a_{s0}^2(\chi_G-\chi_{\max})/N_0$. The solid curves have been plotted for $q_\nu^*=q_{\nu0}=2$, and dashed lines, for $q_\nu^*=q_{\nu0}=3$. Curves *1–3* correspond to $q_{s0}=0.75$, 0.5, and 0.25.

Figure 2 shows the loss in the area estimation accuracy as a function of the ratio $\varepsilon_{q\nu}=(q_\nu^*-q_{\nu0})/q_{\nu0}$ at a fixed value $q_s^*=q_{s0}$. Solid curves have been plot-

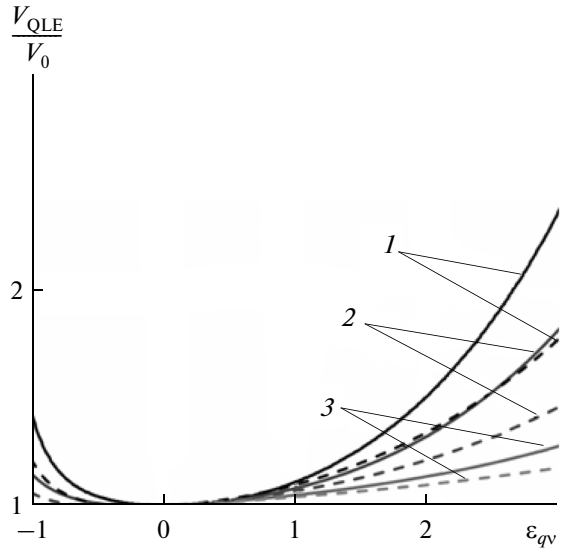

Fig. 2. The loss in the area estimation accuracy vs. presumed values of background intensity.

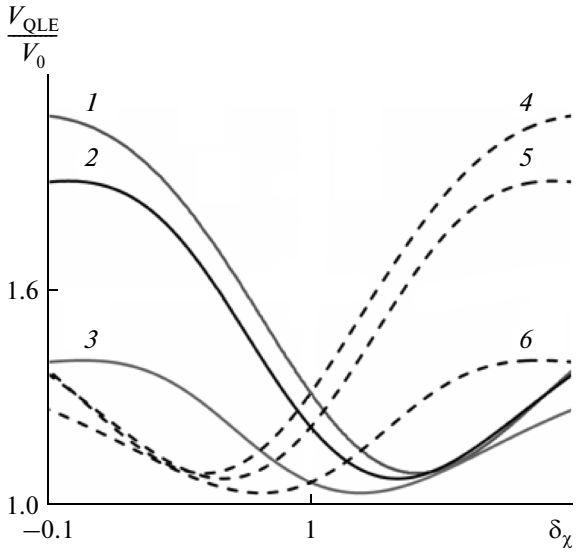

Fig. 3. The loss in the area estimation accuracy vs. parameter $\delta\chi$ with errors of specifying the image and background intensities.

ted for $q_s^* = q_{s0} = 2$, and dashed lines, for $q_s^* = q_{s0} = 3$. Curves *1–3* correspond to $q_{v0} = 0.75$, 0.5, and 0.25.

As follows from Figs. 1 and 2, the errors in the presumed values of the image intensity q_s^* and background intensity q_v^* can substantially reduce the area estimation accuracy. Moreover, the absolute values of the relative errors ε_{qs} and ε_{qv} should not exceed 0.7–0.9. Otherwise, the use of the quasi-likelihood approach for overcoming the parametric prior uncertainty in the image or background intensity can result in a substantial loss in the image area estimation accuracy. The comparison of the solid and dashed curves in Figs. 1 and 2 shows that the sensitivity of the area estimation accuracy to errors in specifying the unknown values of the image and background intensities depends on the distance between these values. In Fig. 1, the background intensity is higher than the image intensity. As a result, an increase in the true value of the image intensity leads to an increase in the loss (solid curves) in the area estimation accuracy. In Fig. 2, the image intensity is greater than the true value of the background intensity. In this case, the increase in the true value of the background intensity also increases the loss (solid curves) in the area estimation accuracy. Thus, the smaller the difference between the true values of the image and background intensities, the larger is the loss in the area estimation accuracy caused by the error of specifying the predicted values.

It should also be noted that errors of specifying the predicted values of the image and background intensities differently affect the area estimation accuracy. For example, the curves in Figs. 1 and 2 have been plotted for $\delta\chi = 0.5$, where $\delta\chi = \chi_{\min}/(\chi_G - \chi_{\max})$ is the ratio of the minimum image area to the minimum background area. It is easy to see that, at such relationship between the areas $\chi_{\min}$, $\chi_{\max}$, and χ_G, the errors in the predicted values of the background intensity lead to smaller losses than the same errors in the predicted image intensity. Nevertheless, if $\delta\chi > 1$, the errors in the presumed background intensity can have a greater effect on the loss in the area estimation accuracy than the errors in the specified presumed value of the image intensity.

Figure 3 for $z_s = z_v = 10$ presents the loss in the area estimation accuracy as a function of the parameter $\delta\chi$. The solid curves have been plotted for $q_v^* = q_{v0} = 2$ and $\varepsilon_{qs} = 1$, and dashed lines, for $q_s^* = q_{s0} = 2$ and $\varepsilon_{qv} = 1$. Thus, curves *1–3* illustrate the loss in the area estimation accuracy versus the errors in the predicted value of the image intensity, and curves *4–6* illustrate the loss in the area estimation accuracy versus the errors of specifying the predicted values of the background intensity. Curves *1–3* correspond to $q_{s0} = 0.75$, 0.5, and 0.25; curves *4–6* correspond to $q_{v0} = 0.75$, 0.5, and 0.25. As follows from the figure, the relationship between the a priori known minimum values of the image area $\chi_{\min}$ and the background area $\chi_G - \chi_{\max}$ affects the sensitivity of the quasi-likelihood algorithm to the errors ε_{qs} and ε_{qv}. Moreover, the $\delta\chi$ determines which of the errors ε_{qs} and ε_{qv} has a greater effect on the image area estimation accuracy.

Let us consider the loss in the area estimation accuracy due to the errors of specifying the values of regular components of the image and background. Figure 4 presents the loss in the area estimation accuracy as a func-

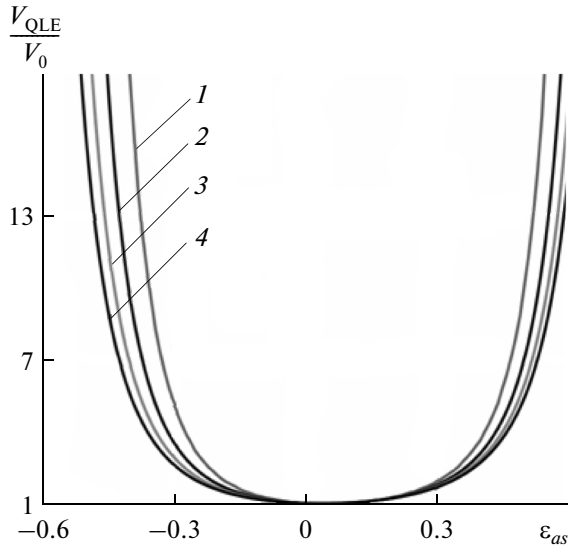

Fig. 4. The loss in the area estimation accuracy vs. presumed value of the regular image component.

tion of the relative error $\varepsilon_{as} = (a_s^* - a_{s0})/a_{s0}$ at $q_s^* = q_{s0} = q_\nu^* = q_{\nu 0} = 0.3$, $a_\nu^* = a_{\nu 0}$, and $z_\nu = 10$. Curves *1–4* correspond to $z_s = 30$, 40, 50, and 60. Figure 5 presents the loss in the area estimation accuracy as a function of the relative error $\varepsilon_{a\nu} = (a_\nu^* - a_{\nu 0})/a_{\nu 0}$ at $q_s^* = q_{s0} = q_\nu^* = q_{\nu 0} = 0.3$, $a_s^* = a_{s0}$, and $z_s = 10$. Curves *1–4* correspond to $z_\nu = 30$, 40, 50, and 60. The ratio $\delta\chi$ in Figs. 4 and 5 was set equal to 0.5.

As follows from Figs. 4 and 5, at the chosen value of the parameter $\delta\chi$, the errors $\varepsilon_{a\nu}$ lead to greater losses in the area estimation accuracy than the same values of the error ε_{as}. At the same time, the errors of specifying the predicted value of the regular image component can substantially reduce the image area estimation accuracy (in particular, in the considered example, for $|\varepsilon_{as}| > 0.3$, the quality of the area estimation abruptly degrades). It should also be noted that the curves in Fig. 4 have been plotted for the case of $z_s > z_\nu$. In this case, a reduction in z_s at a fixed ε_{as} leads to a greater loss in the area estimation accuracy. Similarly, the area estimation accuracy degrades with a reduction in z_ν, when $z_\nu > z_s$, the values of $\varepsilon_{a\nu}$ being fixed (Fig. 5). Therefore, the smaller the difference between z_s and z_ν, the greater is the loss in the area estimation accuracy caused by the errors of specifying the predicted values of the regular components of the image and background.

Figure 6 presents the loss in the area estimation accuracy as a function of the parameter $\delta\chi$ at $q_s^* = q_{s0} = q_\nu^* = q_{\nu 0} = 0.3$. Curves *1–3* have been plotted for $a_\nu^* = a_{\nu 0}$, $z_\nu = 10$, and $\varepsilon_{as} = 0.25$, they characterize the influence of the accuracy of specifying the predicted values of the image and background regular components. Curves *1–3* correspond to $z_s = 30$, 40, and 50. Curves *4–6* have been calculated for $a_s^* = a_{s0}$, $z_s = 10$, and $\varepsilon_{a\nu} = 0.25$, they characterize the influence of the error of specifying the predicted value of the background regular components on the area estimation accuracy. Curves *4–6* correspond to $z_\nu = 30$, 40, and 50.

As follows from Fig. 6, the ratio between the a priori known minimum values of the image area, χ_{min}, and

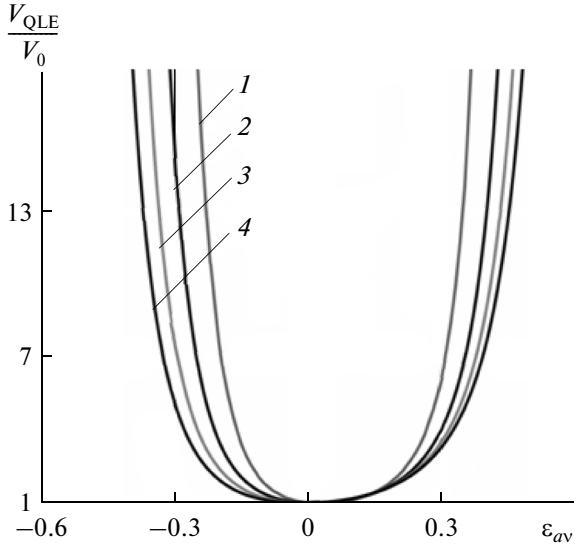

Fig. 5. The loss in the area estimation accuracy vs. presumed value of the regular background component.

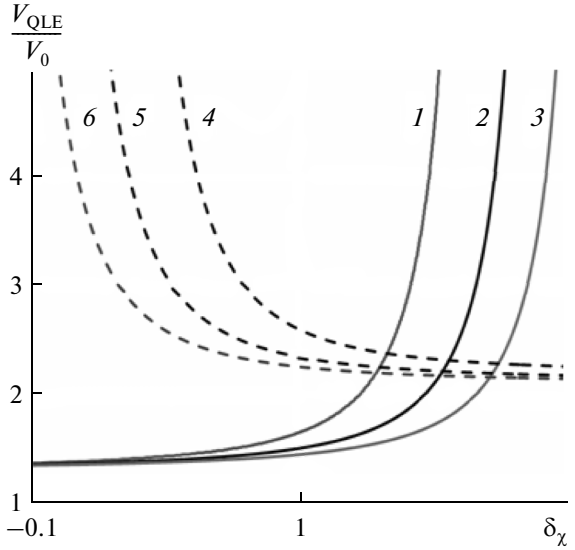

Fig. 6. The loss in the area estimation accuracy vs. parameter $\delta\chi$ with errors of specifying the image and background regular components.

background area, $\chi_G - \chi_{\max}$, can have a noticeable effect on the sensitivity of the quasi-likelihood algorithm of area estimation to the errors ε_{as} and $\varepsilon_{a\nu}$. In this case, the parameter $\delta\chi$ determines which of the errors ε_{as} and $\varepsilon_{a\nu}$ makes a greater effect on the image area estimation accuracy. Extending the results presented in Figs. 3 and 6, we conclude that, at fixed parameters (μ_s, μ_ν, φ), a reduction in $\delta\chi$ leads to a greater influence of the error of specifying the predicted values of the image intensity and background regular component whereas, with an increase in $\delta\chi$, a greater effect is exerted by the errors of specifying the background intensity and the regular image component.

Thus, the accuracy of the quasi-likelihood algorithm for area estimation essentially depends on the accuracy of specifying the predicted values a_s^*, a_ν^*, q_s^*, and q_ν^*. The losses caused by the errors of specifying these quantities can reach substantial values and depend not only on the energy relationships characterizing the signal-to-noise ratio (μ_s, q_{s0}, z_s) or the background-to-noise ratio (μ_ν, $q_{\nu 0}$, z_ν) but also on the ratio between the a priori known minimum values of the image area, $\chi_{\min}$, and background area, $\chi_G - \chi_{\max}$.

The losses in area estimation accuracy can be reduced by replacing the presumed values a_s^*, q_s^*, a_ν^*, and q_ν^* by the their maximum-likelihood estimates [8]. In this case, the maximum likelihood estimate (MLE) of the unknown area has the form

$$\hat{\chi}_{\mathrm{MLE}} = \arg\sup_{\chi} L(\chi),$$
$$L(\chi) = L(\hat{a}_s(\chi), \hat{q}_s(\chi), \hat{a}_\nu(\chi), \hat{q}_\nu(\chi), \chi), \tag{13}$$

where $\hat{a}_s(\chi), \hat{q}_s(\chi), \hat{a}_\nu(\chi), \hat{q}_\nu(\chi) = \arg\max_{a_s, q_s, a_\nu, q_\nu} L(a_s, q_s, a_\nu, q_\nu, \chi)$ is the MLE of the unknown regular components of the image and background relative intensities.

Maximizing (4) and (5), we obtain the explicit form of the estimates $\hat{a}_s(\chi)$, $\hat{q}_s(\chi)$, $\hat{a}_\nu(\chi)$, and $\hat{q}_\nu(\chi)$:

$$\hat{a}_s(\chi) = \frac{X_s(\chi)}{\chi},$$
$$\hat{q}_s(\chi) = \frac{2\chi_{\min}}{\mu_s N_0 \chi}\left[Y_s(\chi) - \frac{X_s^2(\chi)}{\chi}\right] - 1, \tag{14}$$

$$\hat{a}_\nu(\chi) = \frac{X_\nu(\chi)}{\chi_G - \chi},$$
$$\hat{q}_\nu(\chi) = \frac{2(\chi_G - \chi_{\max})}{\mu_\nu N_0 (\chi_G - \chi)}\left[Y_\nu(\chi) - \frac{X_\nu^2(\chi)}{\chi_G - \chi}\right] - 1. \tag{15}$$

Averaging (14) and (15) over the realizations of the observed data at fixed values a_{s0}, q_{s0}, $a_{\nu 0}$, and $q_{\nu 0}$ of all unknown parameters, we find the mathematical expectations $m_{\hat{a}s}(\chi) = \langle \hat{a}_s - a_{s0} \rangle$, $m_{\hat{a}\nu}(\chi) = \langle \hat{a}_\nu - a_{\nu 0} \rangle$, $m_{\hat{q}s}(\chi) = \langle \hat{q}_s - q_{s0} \rangle$, and $m_{\hat{q}\nu}(\chi) = \langle \hat{q}_\nu - q_{\nu 0} \rangle$ and the variances $\sigma^2_{\hat{a}s}(\chi) = \left\langle (\hat{a}_s - \langle \hat{a}_s \rangle)^2 \right\rangle$, $\sigma^2_{\hat{a}\nu}(\chi) = \left\langle (\hat{a}_\nu - \langle \hat{a}_\nu \rangle)^2 \right\rangle$, $\sigma^2_{\hat{q}s}(\chi) = \left\langle (\hat{q}_s - \langle \hat{q}_s \rangle)^2 \right\rangle$, and $\sigma^2_{\hat{q}\nu}(\chi) = \left\langle (\hat{q}_\nu - \langle \hat{q}_\nu \rangle)^2 \right\rangle$ of estimates (14) and (15) for $\mu_s \gg 1$ and $\mu_\nu \gg 1$:

$$m_{\hat{a}s}(\chi) = a_{s0}\frac{\min(\chi_0, \chi)}{\chi} + a_{\nu 0}\frac{\max(0, \chi - \chi_0)}{\chi},$$

$$m_{\hat{a}\nu}(\chi) = a_{s0}\frac{\max(0, \chi_0 - \chi)}{\chi_G - \chi} + a_{\nu 0}\frac{\chi_G - \max(\chi_0, \chi)}{\chi_G - \chi},$$

$$m_{\hat{q}s}(\chi) = \frac{1}{\chi}\Bigg[(1 + q_{s0})\min(\chi_0, \chi) + \left(1 + \varphi q_{\nu 0}\sqrt{\frac{\mu_b}{\mu_s}}\right)\max(0, \chi - \chi_0)\Bigg] - \frac{\chi_{\min}}{\mu_s \chi}\Bigg[\frac{1}{\chi}((1 + q_{s0}) \times \min(\chi_0, \chi) + (1 + q_{\nu 0})\max(0, \chi - \chi_0)) - \frac{2a_{s0}^2}{N_0}\min(\chi_0, \chi) - \frac{2a_{\nu 0}^2}{N_0}\max(0, \chi - \chi_0) + \frac{2}{N_0 \chi}\left(a_{s0}\min(\chi_0, \chi) + a_{\nu 0}\max(0, \chi - \chi_0)\right)^2\Bigg] - 1,$$

$$m_{\hat{q}\nu}(\chi) = \frac{1}{(\chi_G - \chi)}\Bigg[\left(1 + \varphi q_{s0}\sqrt{\frac{\mu_s}{\mu_b}}\right)\max(0, \chi_0 - \chi) + (1 + q_{\nu 0})(\chi_G - \max(\chi_0, \chi))\Bigg] - \frac{(\chi_G - \chi_{\max})}{\mu_\nu (\chi_G - \chi)} \times \Bigg[\frac{1}{(\chi_G - \chi)}((1 + q_{s0})\max(0, \chi_0 - \chi) + (1 + q_{\nu 0})(\chi_G - \max(\chi_0, \chi))) - \frac{2a_{s0}^2}{N_0}\max(0, \chi_0 - \chi) - \frac{2a_{\nu 0}^2}{N_0}(\chi_G - \max(\chi_0, \chi)) + \frac{2}{N_0(\chi_G - \chi)}\left(a_{s0} + a_{\nu 0}(\chi_G - \max(\chi_0, \chi))\right)^2\Bigg] - 1,$$

$$\sigma^2_{\hat{a}s}(\chi) = \frac{1}{\chi^2}\Bigg[\frac{2}{N_0}((1 + q_{s0})\min(\chi_0, \chi) + (1 + q_{\nu 0})\max(0, \chi - \chi_0)) + \left(a_{s0}\min(\chi_0, \chi) + a_{\nu 0}\max(0, \chi - \chi_0)\right)^2\Bigg],$$

$$\sigma^2_{\hat{a}\nu}(\chi) = \frac{1}{(\chi_G - \chi)^2}\Bigg[\frac{2}{N_0}((1 + q_{s0})\max(0, \chi_0 - \chi) + (1 + q_{\nu 0})(\chi_G - \max(\chi_0, \chi))) + (\max(0, \chi_0 - \chi) + a_{\nu 0}(\chi_G - \max(\chi_0, \chi)))^2\Bigg],$$

$$\sigma^2_{\hat{q}s}(\chi) = \frac{\chi^2_{\min}}{\mu_s^2\chi^2}\left\{\frac{2\mu_s}{\chi_{\min}}\left[(1+q_{s0})^2\min(\chi_0,\chi)\right.\right.$$
$$\left.+\left(1+\varphi q_{v0}(2+q_{v0})\sqrt{\frac{\mu_b}{\mu_s}}\right)\max(0,\chi-\chi_0)\right]$$
$$+\frac{2}{\chi^2}\left[(1+q_{s0})\min(\chi_0,\chi)+(1+q_{v0})\max(0,\chi-\chi_0)\right]^2$$
$$-\frac{4}{\chi}\left[(1+q_{s0})^2\min(\chi_0,\chi)+(1+q_{v0})^2\max(0,\chi-\chi_0)\right]$$
$$+4(a_{s0}-a_{v0})^2\left[(1+q_{s0})\min(\chi_0,\chi)\max^2(0,\chi-\chi_0)\right.$$
$$\left.\left.+(1+q_{v0})\min^2(\chi_0,\chi)\max(0,\chi-\chi_0)\right]\right\},$$

$$\sigma^2_{\hat{q}v}(\chi) = \frac{(\chi_G-\chi_{\max})^2}{\mu_v^2(\chi_G-\chi)^2}\left\{\frac{2\mu_v}{\chi_G-\chi_{\max}}\left[\left(1+q_{s0}\varphi(2+q_{s0})\right.\right.\right.$$
$$\left.\left.\times\sqrt{\frac{\mu_s}{\mu_b}}\right)\max(0,\chi_0-\chi)+(1+q_{v0})^2(\chi_G-\max(\chi_0,\chi))\right]$$
$$+\frac{2}{(\chi_G-\chi)^2}\left[(1+q_{s0})\max(0,\chi_0-\chi)+(1+q_{v0})\right.$$
$$\left.\times(\chi_G-\max(\chi_0,\chi))\right]^2-\frac{4}{\chi_G-\chi}\left[(1+q_{s0})^2\right.$$
$$\left.\times\max(0,\chi_0-\chi)-(1+q_{v0})^2(\chi_G-\max(\chi_0,\chi))\right]$$
$$+\frac{8(a_{s0}-a_{v0})^2}{N_0}\left[(1+q_{s0})(\chi_G-\max(\chi_0,\chi))^2\max(0,\chi_0\right.$$
$$\left.\left.-\chi)+(1+q_{v0})(\chi_G-\max(\chi_0,\chi))\max^2(0,\chi_0-\chi)\right]\right\}.$$

Taking into account expressions (14) and (15), we can write log-LRF (13) in the form

$$L(\chi) = L_s(\chi) + L_v(\chi), \tag{16}$$

where

$$L_s(\chi) = \frac{\chi}{N_0}\hat{a}_s^{\,2}(\chi) + \frac{\mu_s\chi}{2\chi_{\min}}\left[\hat{q}_s(\chi)-\ln(1+\hat{q}_s(\chi))\right], \tag{17}$$

$$L_v(\chi) = \frac{\chi_G-\chi}{N_0}\hat{a}_v^{\,2}(\chi)$$
$$+\frac{\mu_v(\chi_G-\chi)}{2(\chi_G-\chi_{\max})}\left[\hat{q}_v(\chi)-\ln(1+\hat{q}_v(\chi))\right]. \tag{18}$$

From the comparison of (16)–(18) and (3)–(5) we conclude that the maximum-likelihood algorithm is more difficult to implement than the quasi-likelihood algorithm.

By subsequent manipulations, we can show that, as the number of degrees of freedom unlimitedly increases, $\mu_s \to \infty$, we have $\sigma_{\hat{q}s}(\chi)/(m_{\hat{q}s}(\chi)+1) \to 0$. Therefore, when $\mu_s \gg 1$, the random function to which the last term in (17) is proportional admits the approximate representation

$$\hat{q}_s(\chi) - \ln(1+\hat{q}_s(\chi))$$
$$\approx m_{\hat{q}s}(\chi)\frac{1+\hat{q}_s(\chi)}{1+m_{\hat{q}s}(\chi)} - \ln(1+m_{\hat{q}s}(\chi)). \tag{19}$$

With allowance for (19), functional (17) can be represented as follows:

$$L_s(\chi) \approx \frac{\chi}{N_0}\hat{a}_s^{\,2}(\chi)$$
$$+\frac{\mu_s\chi}{2\chi_{\min}}\left[m_{\hat{q}s}(\chi)\frac{1+\hat{q}_s(\chi)}{1+m_{\hat{q}s}(\chi)} - \ln(1+m_{\hat{q}s}(\chi))\right]. \tag{20}$$

Let us introduce the normalized random variables with zero mean and unit variance,

$$\xi_{qs}(\chi) = (\hat{q}_s(\chi) - m_{\hat{q}s}(\chi))/\sigma_{\hat{q}s}(\chi),$$
$$\xi_{as}(\chi) = (\hat{a}_s(\chi) - m_{\hat{a}s}(\chi))/\sigma_{\hat{a}s}(\chi)$$

and rewrite expression (20) as

$$L_s(\chi) \approx \frac{\chi}{N_0}\sigma^2_{\hat{a}s}(\chi)\xi^2_{as}(\chi)$$
$$+\frac{\mu_s\chi}{2\chi_{\min}}\frac{\sigma_{\hat{q}s}(\chi)}{1+m_{\hat{q}s}(\chi)}\xi_{qs}(\chi) + \frac{2\chi}{N_0}m_{\hat{a}s}(\chi)\sigma_{\hat{a}s}(\chi)\xi_{as}$$
$$+\frac{\mu_s\chi}{2\chi_{\min}}\left[m_{\hat{q}s}(\chi) - \ln(1+m_{\hat{q}s}(\chi))\right] + \frac{\chi}{N_0}m^2_{\hat{a}s}(\chi).$$

In the obtained expression, let us analyze the behavior of the factors multiplying the random variables $\xi^2_{as}(\chi)$, $\xi_{qs}(\chi)$, and ξ_{as} as $\mu_s \to \infty$. It is easy to see that, as the number of degrees of freedom of the image unlimitedly increases, the factor $\mu_s\chi\sigma_{\hat{q}s}(\chi)/2\chi_{\min}(1+m_{\hat{q}s}(\chi))$, multiplying the random variable $\xi_{qs}(\chi)$, unlimitedly increases whereas the product $2\chi m_{\hat{a}s}(\chi)\sigma_{\hat{a}s}(\chi)/N_0$, multiplying ξ_{as}, and the product $\chi\sigma^2_{\hat{a}s}(\chi)/N_0$, multiplying the random variable $\xi^2_{as}(\chi)$, are independent of μ_s and take finite values. Therefore, with an unlimited increase in the number of degrees of freedom μ_s, the distribution of functional (17) is characterized by the random component of the image intensity estimate $\xi_{qs}(\chi)$. Using the results of [12], we can show that, as $\mu_s \to \infty$, the law of distribution of the quantity $\xi_{qs}(\chi)$ tends to a Gaussian one. Therefore, functional (17) at a fixed value of the unknown area may be considered a Gaussian random process.

In a similar manner, we find that, as $\mu_v \to \infty$, functional (18) admits the approximation

$$L_v(\chi) \approx \frac{\mu_v(\chi_G-\chi)}{2(\chi_G-\chi_{\max})}\left[\frac{1+\hat{q}_v(\chi)}{1+m_{\hat{q}v}(\chi)} + m_{\hat{q}v}(\chi)\right.$$
$$\left.-1-\ln(1+m_{\hat{q}v}(\chi))\right] + \frac{\chi_G-\chi}{N_0}\hat{a}^2_v(\chi)$$

and is an asymptotically Gaussian random process. Then, as was shown in [7], in the vicinity of the true value of the parameter, χ_0, log-LRF $L(\chi)$ (16) as a function of the unknown area χ may be approximately considered a Gaussian Markov process. Using the method from [9], we find the drift coefficient $K_{1\mathrm{MLE}}(\chi)$ and diffusion coefficient $K_{2\mathrm{MLE}}(\chi)$ of process (6):

$$\begin{aligned} K_{1\mathrm{MLE}}(\chi) &\approx K_{1\mathrm{QLE}}(a_{s0}, q_{s0}, a_{v0}, q_{v0}, \chi), \\ K_{2\mathrm{MLE}}(\chi) &\approx K_{2\mathrm{QLE}}(a_{s0}, q_{s0}, a_{v0}, q_{v0}, \chi), \end{aligned} \quad (21)$$

where the coefficients $K_{1\mathrm{QLE}}$ and $K_{2\mathrm{QLE}}$ are defined by (6) and (7), respectively.

Relationships (21) imply that the characteristics of the area estimate with the use of MLE of unknown image and background regular components asymptotically (as $\mu_s \to \infty$, $\mu_v \to \infty$) coincide with the characteristics of the area estimate with the use of a priori known image and background parameters. Thus, the curves in Figs. 1–6 also characterize the loss in the area estimation accuracy if the quasi-likelihood estimates a_s^*, q_s^*, a_v^*, and q_v^* are used instead of the MLE $\hat{a}_s$, $\hat{q}_s$, $\hat{a}_v$, and $\hat{q}_v$. According to Figs. 1–6, the maximum-likelihood algorithm makes it possible to increase the accuracy of area estimation with unknown non-informative parameters of the image and background. At the same time, the use of the simpler quasi-likelihood algorithm for area estimation may be appropriate if the relative errors of specifying the unknown intensities of the image and background regular components are within ten percent. Depending on the specified conditions, the particular quantitative recommendations on the application of quasi-likelihood algorithm can be formulated on the basis of the expressions obtained above.

This work was supported by the Russian Science Foundation, project no. 14-49-00079.

REFERENCES

1. B. B. Mikhailov and E. A. Devyaterikov, Nauch.-Tekh. Vedomosti SPbGPU. Ser.: Inf., Telekommun. Upravlenie, No. 5(181), 103 (2013).
2. A. V. Nguen and B. B. Mikhailov, Robototekh. Tekhnich. Kibernetika, No. 1(2), 65 (2014).
3. G. I. Peretyagin, Avtometriya, No. 6, 42 (1984).
4. R. Kashyap and R. Chellappa, IEEE Trans. Inf. Theory **29**, 60 (1983).
5. A. A. Bychkov and V. A. Pon'kin, Avtometriya, No. 4, 33 (1992).
6. C. Bouman and K. Sauer, IEEE Trans. Image Process. **2**, 296 (1993).
7. A. P. Trifonov and Yu. N. Pribytkov, Avtometriya **46** (2), 49 (2010).
8. E. I. Kulikov and A. P. Trifonov, *Estimation of Parameters of Signals on the Background of Disturbance* (Sovetskoe Radio, Moscow, 1978) [in Russian].
9. A. P. Trifonov, E. P. Nechaev, and V. I. Parfenov, *Detection of Stochastic Signals with Unknown Parameters* (Voronezh. Gos. Univ., Voronezh, 1991) [in Russian].
10. *Applied Theory of Random Processes and Fields*, Ed. by K. K. Vasil'ev and V. A. Omel'chenko (Ul'yanovsk. Gos. Tekh. Univ., Ul'yanovsk, 1995), pp. 164–214 [in Russian].
11. A. P. Trifonov and Yu. S. Shinakov, *Joint Recognition of Signals and Estimation of Their Characteristics on the Background of Disturbance* (Radio i svyaz', Moscow, 1986) [in Russian].
12. A. P. Trifonov and Yu. N. Pribytkov, Izv. Vyssh. Uchebn. Zaved., Radioelektron. **57** (2), 43 (2014).

Translated by E. Chernokozhin